

CHARGING MANAGEMENT PROTOCOL FOR NEAR FIELD COMMUNICATION CHARGING

Ham Hock Ling^{a,b}, Akaa Agbaeze Eteng^{a*}, Chee Yen Leow^a, Sharul Kamal Abdul Rahim^a, Beng Wah Chew^b

^aWireless Communication Center, Universiti Teknologi Malaysia, 81310, UTM Johor Bahru, Johor, Malaysia

^bIntel Microelectronics, Halaman Kampung Jawa, 11900 Penang, Malaysia

Article history

Received

23 June 2015

Received in revised form

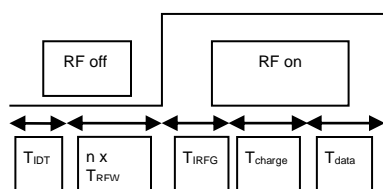
14 November 2015

Accepted

23 January 2016

*Corresponding author
aeakaa2@live.utm.my

Graphical abstract



Abstract

The current multiplicity of mobile communication devices has provided an impetus for the research into new mechanisms to supplement battery charge. Wireless charging is a solution that serves to eliminate the cable requirements of typical battery charging implementations. Numerous wireless charging implementations are based on inductive coupling, similar to existing non-radiative short range communication systems. This study proposes incorporating a charge management protocol into the existing Near Field Communication Interface and Protocol-1 (NFCIP-1) specification to achieve NFC-enabled wireless charging. To this end, the original NFCIP-1 protocol has been modified through a time-sharing arrangement to support a charging task within the protocol cycle. Simulations of the modified protocol cycle were implemented using an appropriate battery model and charging algorithm. Numerical results show that the modified protocol is able to charge the target battery with minimum communication overhead. Satisfactory performance is also observed for charging up to 2 target devices in a single session.

Keywords: NFCIP-1; charging; simulation; protocol; charge management; constant-current/constant-voltage

© 2016 Penerbit UTM Press. All rights reserved

1.0 INTRODUCTION

The development of wireless charging technologies has elicited considerable research interest in recent times. The proliferation of mobile gadgets has accentuated the need for the provision of alternatives to the traditional cable-dependent battery charging arrangements. Although wireless power transmission is an old idea, it has only recently been applied to the deployment of wireless charging infrastructure. The most notable low-power wireless charging deployment is the Qi standard, which is based on inductive coupling at 110 kHz – 205 kHz¹.

Traditional inductive coupling-based wireless charging requires the use of high Q-factor coils to intercept the magnetic field from a charging station. Useful power extracted from the intercepted

magnetic flux is then used to drive battery charging circuits. Apart from its use in power delivery, inductive coupling is also used to facilitate data transfers in non-radiative short range systems, such as Radio Frequency Identification (RFID) and Near Field Communication (NFC) at 13.56 MHz²⁻⁴.

NFC technology presents a convenient platform for e-transactions, and is projected to be incorporated in about 863 million mobile phones by the end of 2015⁵. With wireless charging deployments aiming for similar market penetration, the trend is for handsets to include both NFC and wireless charging hardware. The need, therefore, arises for the integration of both solutions to minimize hardware redundancy, production costs, and device form-factors.

2.0 PROTOCOL DESIGN

The NFC Interface and Protocol-1 (NFCIP-1)⁶ specifies the radio frequency interface, and communication modes, for inductive coupled devices operating at 13.56 MHz. The general protocol, shown in Fig. 1, consists of 5 stages. Stage A is the initialization protocol, which begins with the initial Radio Frequency Collision Avoidance (RFCA), followed by Single Device Detection (SDD), mode initiation, and choosing of transfer speeds. The choice of operating mode (active or passive) is determined by the higher-level application employing the NFCIP-1 for communication. Stage B is the protocol activation stage, which involves an exchange of attributes (ATR) such as bit-rate and payload length between the paired devices. Stage C is an optional Parameter Select (PSL) stage, which can be invoked by the initiator device to alter parameters of subsequent protocol steps. Stage D is the Data Exchange Protocol (DEP), which allows the initiator device exchange data with the target device. Stage E is the de-activation stage, involving the De-Select (DSL) and Release protocols (RLS), effectively terminating the transaction between paired devices, and returning them to their initial states. Stages B – E are collectively described as the NFCIP-1 transport protocol⁶.

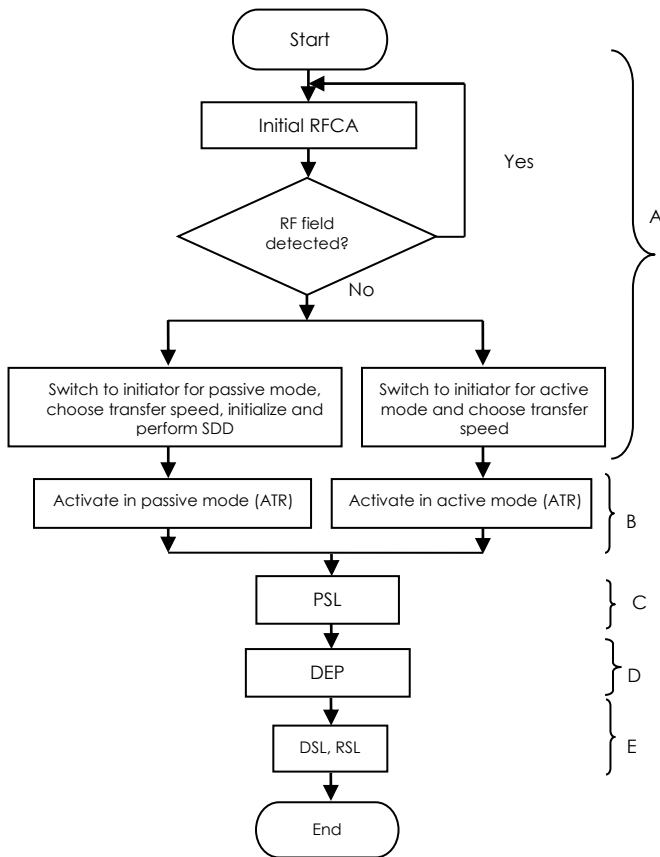


Figure 1 General Flow of NFCIP-1⁶

The implementation of a charging step requires a time-sharing arrangement with minimal modification to the original protocol cycle. The proposed modification would be such as not to interrupt a session by triggering a timeout exception along any step in the original protocol sequence. Assuming a passive mode NFC interaction, this is achieved by inserting the charging step before the issuance of the first command by the session initiator, that is, between the initial RFCA and SDD tasks. The charging duration (T_{charge}) is inserted between the initial guard time upon switching on the RF field (T_{IRFG}), and the start of data transfer (T_{data}), as shown in Fig. 2.

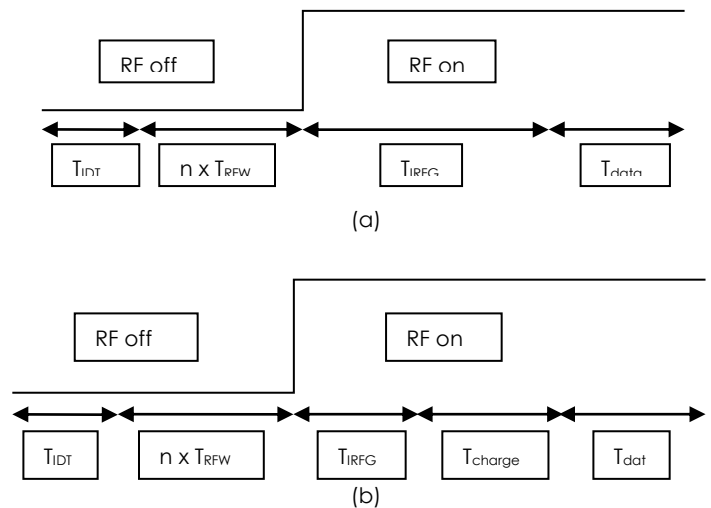


Figure 2(a) Original⁶ and (b) Modified initial RFCA

T_{IDT} is an initial delay ($T_{IDT} > 4096/f_c$), T_{RFW} is the RF waiting time ($512/f_c$), where $f_c = 13.56$ MHz and $0 \leq n \leq 3$. The NFCIP-1 protocol specifies a minimum threshold of 5 ms for the interval between the end of $n \times T_{RFW}$ and the start of T_{data} . Since no maximum time limit is imposed, an extension of this interval through the inclusion of T_{charge} can be handled with the least compromise to the performance of the protocol.

For the proposed NFC charging session, the first cycle is based on the original NFCIP-1 specification, allowing the charging device to obtain information about the target devices. In subsequent cycles, the charger implements the modified protocol to charge the target devices. Hence, the protocol sequence in a session is:

RFCA → SDD → ATR → DEP → RLS → RFCA → CHARGE → SDD → ATR → DEP → RLS → RFCA → CHARGE → ...

A sequence diagram illustrating the command sequence from the first protocol cycle to the first charge operation is shown in Figure 3.

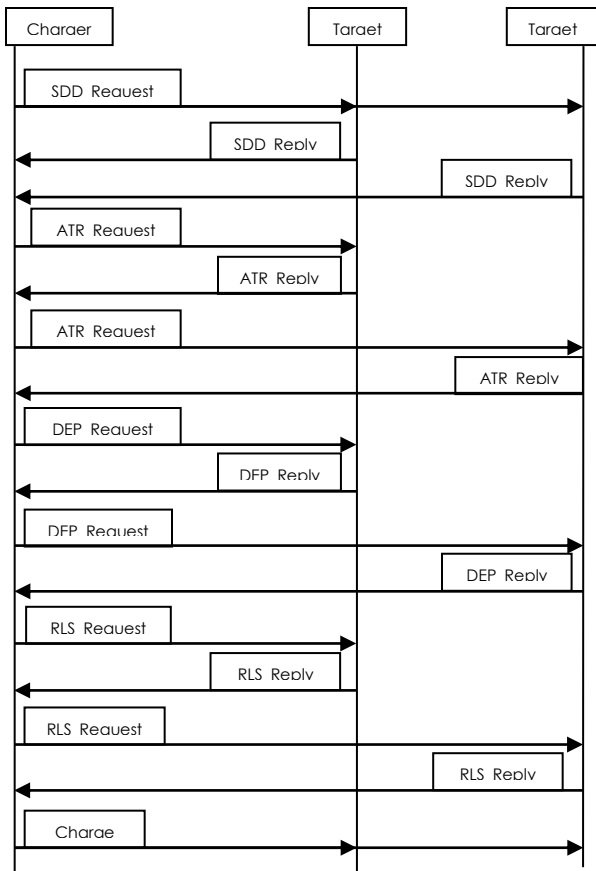


Figure 3 Sequence diagram illustrating protocol flow to charge 2 target devices

3.0 SIMULATION MODELING

3.1 Battery Model

A battery model proposed by Chen and Rincon-Mora⁷ is chosen for the simulation study. This model, shown in Figure 4, is compatible with low-power lithium-ion batteries, which are found in numerous mobile phones. In addition, the model is computationally tractable. The battery model parameters are computed as described in Chen and Rincon-Mora⁷. R_{int} , which is external to the battery model, is the internal circuit resistance of the charging circuit, mainly due to wire resistance. V_{charge} and I_{charge} are the charging voltage and current for a particular battery, computed as functions of model currents I_{C1} and I_{C2} . These model currents are likewise computed as functions of the RC network – $R_{transient_s}$, $R_{transient_L}$, $C_{transient_s}$, $C_{transient_L}$, whose values have been experimentally extracted, along with V_{oc} and R_{series} , for lithium-ion batteries in Chen and Rincon-Mora⁷.

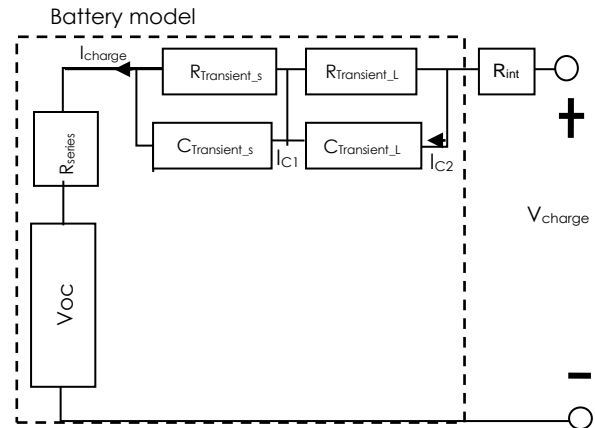


Figure 4 Full charging circuit

3.2 Charging Algorithm

The charging algorithm employed is a modified constant-current/constant-voltage (CC/CV) algorithm⁸ for ease of implementation. The constant current charge rate is set to 1C, and the constant voltage is set to 4.2 V, for a battery life cycle of 400 cycles. The algorithm is modified, as illustrated in Figure 5, by the inclusion of a testing of the state-of-charge (SOC) condition prior to the termination, or otherwise, of constant voltage charging. Hence, charging is terminated either when the charging current is less than 0.05C or when the SOC is greater than or equal to 1.

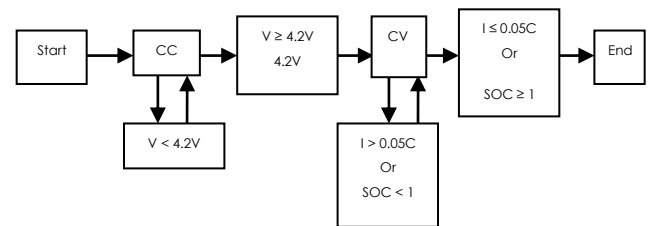


Figure 5 Modified CC/CV charging algorithm

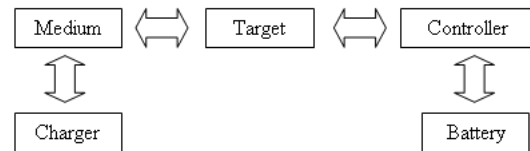


Figure 6 Architecture of simulation programme

3.3 Simulation Program

The structure of the simulation model is shown in Figure 6. The charger communicates with the target device through medium. The target then issues a command to the controller to charge the battery. The program was implemented in C++, with the following assumptions made in running the simulations:

1. Data sent by the target or the initiator is error-free.
2. The target always replies the request from the initiator with correct response.
3. The target always responds before time out occurs.
5. No chaining is used in the DEP stage.
6. The ATR stage does not contain general bytes.
7. Target and initiator have same payload length during DEP stage.
9. The bit rate for NFC is 424 k bits/s.
10. The target has zero power up time.

4.0 RESULTS AND DISCUSSION

4.1 Charging Algorithm

Simulation studies of the chosen CC/CV charging algorithm were undertaken under different operating conditions. First, the effect of battery capacity on charging parameters is examined. R_{int} is assumed to be 0Ω , the ambient temperature was $28 \text{ }^\circ\text{C}$, while the charging rate is $1C$.

Figure 7 shows the charging power with time for different battery capacities. From the figure, it can be observed that the charging power is proportional to the battery capacity. If the battery capacity is doubled, the charging power is doubled also.

In Figure 8, it can be observed that the simulated battery capacities all require about 3600 seconds to fully charge. Hence, while the charging power requirement depends on the battery capacity, the charging time is independent of the battery capacity provided the charging power is adjusted according to the battery capacities.

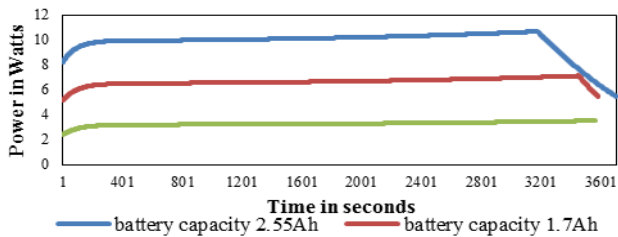


Figure 7 Charging power vs battery charging time for different battery capacities

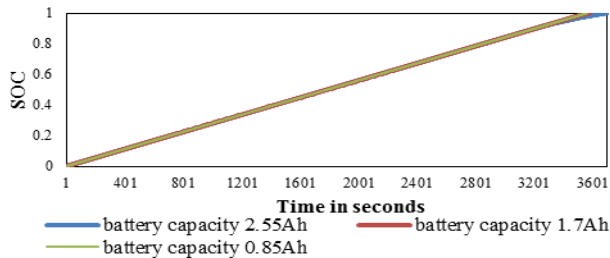


Figure 8 SOC vs. battery charging time for different battery capacities

Next, the effect of different charging currents on the charging power with time is studied. The battery capacity is assumed to be 0.85 Ah , while R_{int} is 0Ω at an ambient temperature of $28 \text{ }^\circ\text{C}$. Fig. 9 shows the relationship between charging power and time with different charging currents. Fig. 10 demonstrates the SOC with time with different charging currents. From these two figures, it is evident that battery charging time is inversely proportional to the charging current. Faster charging is achieved at the price of higher charging power requirements. However, since energy is the product of power and time, the total energy requirement is the same, irrespective of the charging current used.

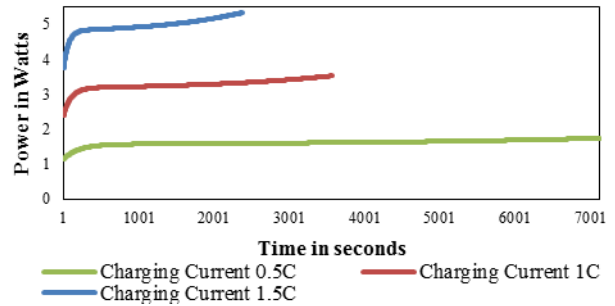


Figure 9 Charging power vs. battery charging time for different charging current values

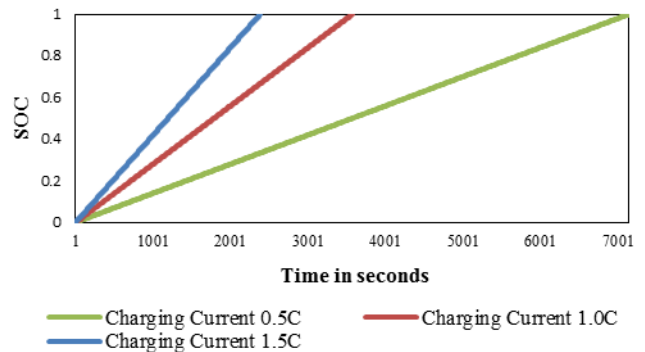


Figure 10 SOC vs. battery charging time for different charging currents

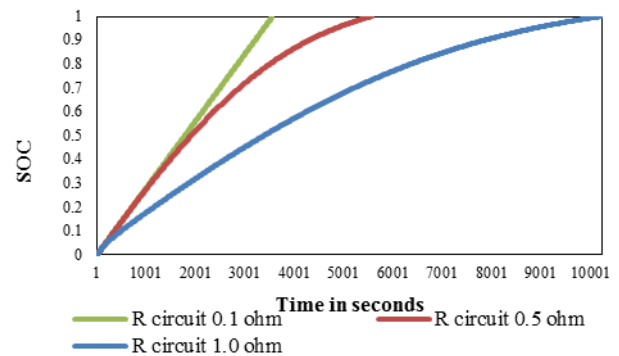


Figure 11 SOC vs. battery charging time with various values of circuit R_{int}

Figure 11 shows the effect of different internal circuit resistances R_{int} on the SOC characteristic with time. With a charging current of 1C and battery capacity of 0.85 Ah, it is observed that increased resistance makes it more difficult to fully charge the battery.

On the basis of the simulated results, the proposed charge management scheme for NFC charging is based on a charging current of 1C, battery capacity of 0.85 Ah, and a pragmatic circuit resistance value of 1Ω .

4.2 Protocol Performance

In order to evaluate the performance of the proposed charging protocol, three issues are studied. The first concerns the relationship between the communication overhead time and charging time when a single device is being charged. This relationship is then studied with two devices being charged simultaneously. The third study focus is the link power profile while charging.

Figure 12 shows the ratio of communication time (blue) to charging time (purple) with one target device in interaction with an initiator. There is an increase in the percentage of effective charging time as the charging duration (T_{charge}) increased. When the charging duration (T_{charge}) is 10 seconds, 92% of the total time is used for charging. Further increase of the charging duration would not result in a significant boost to the charging efficiency, as only eight percent of the total time is left for any further improvement.

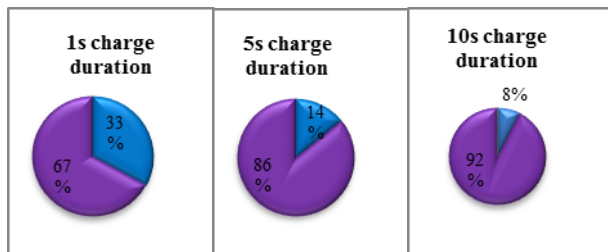


Figure 12 Ratio of effective charging time over total time used

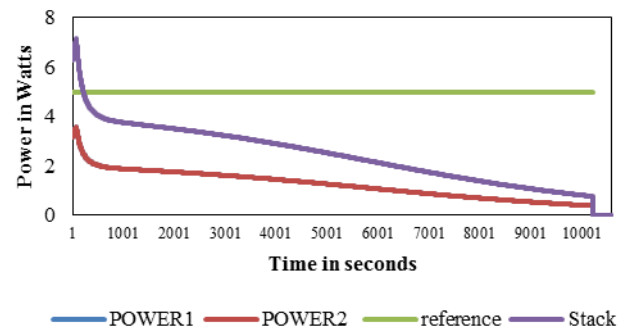
The total time to charge target devices is the sum of the battery charging time and the total communication time, assuming there is continuous NFC data interaction throughout the duration of the charging operation. The battery charging time is 10235 seconds. On the other hand, the total communication time is the sum of the times spent by the charger and targets in executing the NFC protocol. As shown in Table I, using a T_{charge} value of 10 seconds, the total time to charge the battery of a single target device is found to be about 11068 seconds (about 3 hours 5 minutes). For this case, the total communication time is found to be about 833 seconds. However, when charging 2 target devices, the total communication time increased to about

1845 seconds. As a consequence, the total time to charge two target devices increased to about 12080 seconds (about 3 hours 21 minutes). It is expected that the total time will increase with the charging of more target devices.

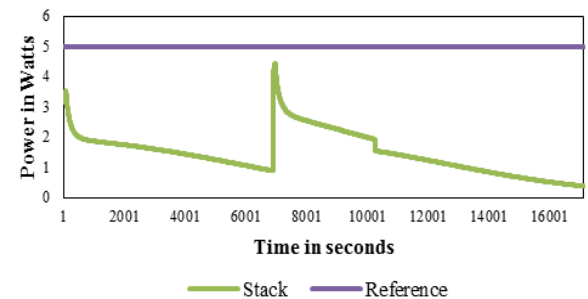
Table 1 Communication time and total time for charging target devices

Charge Target r	Communication Time (secs)		Total Communicati on Time (secs)	Charge Time (secs)	Total Time (secs)
	Target1	Target2			
13.078	820.014	-	833.092	10235	11068.092
20.053	932.857	892.236	1845.146	10235	12080.146

Fig. 13 shows the power demand from the charger with time. Although, conceptually, the battery charger is designed for a maximum charging power of 5 W, the total power drawn to charge 2 target devices initially shoots up beyond 7 W. This behavior can be observed in the power profile shown in Fig. 13 (a).



(a)



(b)

Figure 13 Power demand vs time (a) without power management (b) with power management

This overshoot in the power profile can be attributed to the lack of a power management scheme in the charger. Hence, with a target power demand greater than can be delivered by the

charger, both targets will compete to appropriate all available charging power, resulting in circuit instabilities.

To address this concern, a simple power management algorithm is introduced to the system. Fig. 14 shows the flow chart for this algorithm. To implement this algorithm, the charger collects information about the targets, such as, battery SOC, battery capacity, or charging power needed. The charger then decides which target to charge, and which not to charge yet. The charger needs to finish the computation and assignment before the target times out. Consequently, only one target device charges at each point in time.

With the implementation of the algorithm, the total power demand from the charger does not exceed the 5 W limit, as shown in Fig 13 (b). The drawback of the power management algorithm, however, is an increase in the battery charging time to 17001 seconds.

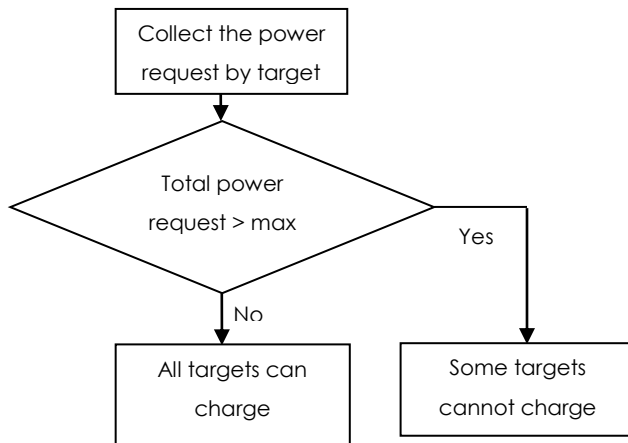


Figure 14 Simple power management algorithm

5.0 CONCLUSION

This paper has presented a modification of the NFCIP-1 protocol to support battery charging. The key protocol modification is in inserting a charging step between the end of the RFCA and the beginning of the SDD tasks initiated by the NFC session initiator. The CC/CV charging algorithm is found to be suitable for the charging task, allowing for a reasonable battery charging time for a single target device. Although 2 target devices could be

charged in parallel, this results in an increase in the charging time, and the charging power demand. To counteract the increased power demand, a charge management algorithm is suggested to ensure the demanded power is within the capacity of the battery charger. The numerical results obtained in this study reveal the potential for the implementation of viable NFC-enabled wireless charging solutions.

Acknowledgement

This work was supported by the Collaborative Research in Engineering, Science and Technology (CREST) fund, Malaysia, under grant number 4B151, the Ministry of Science, Technology and Innovation under vote no. 4S079, and Universiti Teknologi Malaysia Research University Grant under vote no. 05H39.

References

- [1] Hui, S. Y. 2013. Planar Wireless Charging Technology for Portable Electronic Products and Qi. *Proc. IEEE*. 6(101): 1290–1301.
- [2] Innovision Research & Technology plc. 2013. *Near Field Communication in real world - Part I*. [Online]. [Accessed on December 20, 2013]. From: http://members.nfc-forum.org/resources/white_papers/.
- [3] Innovision Research & Technology plc. *Near Field Communication in Real World - Part II*. [Online]. [Accessed on December 20, 2013]. From: http://members.nfc-forum.org/resources/white_papers/.
- [4] Innovision Research & Technology plc. *Near Field Communication in real world - Part III*. [Online]. [Accessed on December 20, 2013]. From: http://members.nfc-forum.org/resources/white_papers/.
- [5] Strommer, E., Jurvansuu, M., Tuikka, T., Ylisaukko-oja, A., Rapakko, H., Vesterinen, J. 2012. NFC-Enabled Wireless Charging. *Near Field Communication Workshop (NFC 2012), 4th International*. Helsinki, Finland. 13 March 2012. 36–41.
- [6] ECMA International. 2013. *NFCIP -1*. Europe: ECMA International.
- [7] Thanh T. V., Weixiang S., Kapoor, A. 2012. Experimental comparison of charging algorithms for a lithium-ion battery. *Power and Energy Conference (IPEC), 10th International*. Ho Chi Minh, Vietnam. 12–14 December 2012. 207–212
- [8] Weixiang, S., Thanh, T. V., Kapoor, A. 2012. Charging Algorithms Of Lithium-Ion Batteries: An Overview. *Industrial Electronics and Applications Conference (ICIEA), 7th IEEE*. 18–20 July 2012. 1567–1572.